APPENDIX C

Appl. No. 10/781,979
Filed: February 19, 2004
Attorney's Docket No. 045600/274147
Group Art Unit 1638
Examiner: Anne R. Kubelik

Mutations at Domain II, Loop 3, of *Bacillus thuringiensis* CryIAa and CryIAb δ-Endotoxins Suggest Loop 3 Is Involved in Initial Binding to Lepidopteran Midguts*

Francis Rajamohan‡, Syed-Rehan A. Hussain§, Jeffrey A. Cotrill‡, Fred Gould¶, and Donald H. Dean‡§‖

From the ‡Department of Biochemistry, §Molecular, Cellular and Developmental Biology Program, The Ohio State University, Columbus, Ohio 43210 and the ¶Department of Entomology, North Carolina State University, Raleigh, North Carolina 27695

Alanine substitutions of loop 3 residues, [438]SGF-SNS[443], of CryIAb toxin were constructed to study the functional role of these residues in receptor binding and toxicity to *Manduca sexta* and *Heliothis virescens*. Experiments with trypsin and insect gut juice enzyme digestions of mutant toxins showed that these mutations did not produce any gross structural changes to the toxin molecule. Bioassay data showed that mutant G439A (alanine substitution of residue Gly[439]) and F440A significantly reduced toxicity toward *M. sexta* and *H. virescens*. In contrast, mutants S438A, S441A, N442A, and S443A were similar or only marginally less toxic (2–3 times) to the insects compared to the wild-type toxin. Binding studies with brush border membrane vesicles prepared from *M. sexta* and *H. virescens* midgut membranes revealed that the loss of toxicity of mutants G439A and F440A was attributable to substantially reduced initial binding. Consistent with the initial binding, mutants G349A and F440A showed 3.5 times less binding to *M. sexta* and *H. virescens* brush border membrane vesicles, although the off-rate of bound toxins was not affected. The role of hydrophobic residue, Phe[440], is distinctly different from our previous observation that alanine substitution of Phe[371] at loop 2 of CryIAb did not affect initial binding but reduced irreversible association of the toxin to the receptor or membrane toward *M. sexta* (Rajamohan, F., Alcantara, E., Lee, M. K., Chen, X. J., and Dean, D. H. (1995) *J. Bacteriol.* 177, 2276–2282). Likewise, deletion of relatively hydrophobic CryIAa loop 3 residues, [440]AAGA[443] (D3a), resulted in reduced toxicity to *Bombyx mori* (>62 times less) and *M. sexta* (28 times less). The loss of toxicity was correlated with reduced initial binding to midgut vesicles prepared from these insects. However, alanine substitution of residues [437]LSQ[439] (A3a), contiguous to loop 3, altered neither toxicity nor receptor binding toward *B. mori* or *M. sexta*. These results suggest that the loop 3 residues of CryIAb and CryIAa toxins establish hydrophobic interactions with the receptor molecule, and mutations at these hydrophobic residues affect initial binding.

The insecticidal crystal proteins (ICPs or δ-endotoxins) produced by *Bacillus thuringiensis* are of great scientific interest because of their potency and specificity against a wide range of agronomically important insect pests and vectors of human diseases (1). The bacteria express the protein during the late growth phase as a protoxin (120–140 kDa for CryI types), which accumulates in the cell as crystals of various shapes (2). Upon ingestion of the crystals, the protoxin is solubilized and activated into a 60–65-kDa protease-resistant toxin by the proteolytic enzymes present in the larval midgut. The activated toxin binds to specific receptors (toxin-binding proteins) located on the midgut brush border membrane of the columnar cells (3, 4). Binding of toxin to the receptor generates ion channels across the midgut apical membrane, leading to death of the cells (5–7) and finally of the larvae.

The x-ray crystal structure of a lepidopteran active δ-endotoxin, CryIAa, has been recently determined by Grochulski *et al.* (8). This structure supports the three domain structure of CryIIIA, a coleopteran active toxin, determined by Li *et al.* (9). In summary, domain I is composed of seven α-helixes, which may be involved in the membrane spanning activity of the toxin. Mutations in domain I of CryI type toxins can inhibit toxicity and channel forming activity (10, 11). Domain II has three antiparallel β-sheets, connected to each other with surface-exposed loops of different lengths, oriented in parallel with the helical bundle of domain I. These loops are attractive candidates for a role in receptor recognition and binding. Domain III, a bundle of β-sheets, has been reported to be involved in ion-channel activity (12), receptor binding (13), and structural stability (14). CryIAb toxin is believed to have a similar structure as CryIAa, since it shares about 89% amino acid sequence identity with CryIAa toxin (8).

In many cases, *in vitro* binding studies using ^{125}I-labeled toxins and midgut brush border membrane vesicles (BBMV)[1] isolated from susceptible and resistant insect larvae have shown a direct correlation between insect toxicity and binding (15, 16). Recent studies on binding kinetics suggest a two-step process (reversible and irreversible) for Cry toxins with several lepidopteran insects (17, 18). Interestingly, a direct correlation between toxicity and the rate constant for irreversibly bound toxin has been observed (17). Recent progress on the identification and purification of insect midgut toxin-binding (receptor) molecules suggest 120- and 210-kDa proteins from *Manduca sexta* as binding proteins for CryIAc and CryIAb toxins, respectively (19, 20). In gypsy moth BBMV, CryIAa, and CryIAb toxins bind to a 210-kDa protein and CryIAc binds to a 120-kDa amino peptidase-N (13, 21).

The domain II loop residues of Cry toxins have been targeted

---

[1] The abbreviations used are: BBMV, brush boarder membrane vesicle; PAGE, polyacrylamide gel electrophoresis.

by site-directed mutagenesis and membrane binding assays to investigate the molecular basis for the action of δ-endotoxins. Wu and Dean (22) mutated the loop residues of CryIIIA and observed that loops 1 and 3 are involved in receptor binding. Recent studies by Rajamohan *et al.* (18, 23) on CryIAb showed that loop 2 residues, [368]RRP[370], are involved in initial receptor binding, while residues Phe[371] and Gly[374] of the same loop are largely involved in irreversible binding of the toxin to *M. sexta*. In earlier reports, deletion of a portion of CryIAa loop 2 (residues 365–371) removed nearly all toxicity and initial binding to *Bombyx mori* (24), while mutations in loop 1 showed no effect on initial binding (25). These studies establish the significance of domain II loop residues in receptor binding. In the present communication we target another loop in domain II, loop 3, of CryIAa and CryIAb toxins and analyze its functional role in receptor binding and toxicity. We demonstrate that either deletion or alanine substitution of loop 3 amino acids, especially affecting hydrophobic residues, of CryIAa and CryIAb toxins significantly affect the initial binding ability to *M. sexta*, *B. mori*, and *Heliothis virescens* membrane vesicles and reduce their potency to the target insects.

MATERIALS AND METHODS

Site-directed Mutagenesis—The oligonucleotides used for site-directed mutagenesis were kindly provided by Dr. Takashi Yamamoto, Sandoz Agro Inc., Palo Alto, CA. A uracil-containing template of *cryIAa* and *cryIAb* genes was obtained by transforming *Escherichia coli* CJ236 (Bio-Rad) with pOSM1313 (26) and pSB033b (18), respectively. The site-directed mutagenesis procedure followed the manufacturer's manual (Muta-Gene M13 *in vitro* mutagenesis kit; Bio-Rad). DNA sequencing was carried out by the method of Sanger *et al.* (27) following the manufacturer's (U. S. Biochemical Corp.) instructions. Fine chemicals and restriction enzymes were purchased from Boehringer Mannheim.

Expression and Purification of Toxin—Mutant and wild-type δ-endotoxins were expressed in *E. coli* MV1190 and were purified as described previously (18). The purified crystal protein was solubilized in crystal solubilization buffer (50 mM Na_2Co_3, pH 9.5, 10 mM dithiothreitol) at 37 °C for 3 h. Activation of the solubilized protoxin was carried out by treating with 2% (by mass) trypsin (Sigma) at 37 °C for 5 h and was analyzed by sodium dodecyl sulfate-10% polyacrylamide gel electrophoresis (PAGE).

Protein Determination—Protein concentrations of toxins and BBMV were determined with the Coomassie protein assay reagent (Pierce) using bovine serum albumin as a standard.

Protease Digestions and Western Blotting—Insect gut enzyme digestion of mutant and wild-type proteins was performed by incubating the toxin with freshly prepared gut enzymes at 37 °C for 3 h as described before (18). The final digested products were separated on SDS-10% PAGE, transferred onto polyvinylidene difluoride membrane (Bio-Rad); treated with anti-CryIAa or CryIAb serum and the blot was processed and developed as described previously (18).

Toxin Iodination—Twenty μg of trypsin-activated toxin were labeled using 1 mCi of [125]I (Dupont) and one IODOBEAD (Pierce) following the manufacturer's directions. Free iodine was separated from the toxin using a prepacked Excellulose GF-5 column (Pierce) as described previously (18). The specific activities of labeled CryIAa, A3a, D3a, CryIAb, S438A, G439A, F440A, S441A, N442A and S443A were 1.9, 1.9, 1.7, 2.1, 1.9, 2.3, 1.4, 1.5, 1.8, and 1.6 mCi/mg, respectively.

Preparation of BBMV—Insect midguts were prepared as described previously (12) and were stored at liquid nitrogen or at −70 °C until use. BBMV were prepared by the differential magnesium precipitation method as modified by Wolfersberger *et al.* (28). The final vesicles were resuspended in binding buffer (8 mM $NaHPO_4$, 2 mM KH_2PO_4, 150 mM NaCl, pH 7.4, containing 0.1% bovine serum albumin) to a final protein concentration of 1 mg/ml and stored at −70 °C until use.

Toxicity Assays—*B. mori* eggs were kindly supplied by R. E. Milne, Forest Pest Management Institute, Sault Ste. Marie, Canada. The eggs were hatched and raised to third instar on mulberry leaves. A 5.0-μl total volume of each toxin dilution (diluted in phosphate-buffered saline, 8 mM Na_2HPO_4, 2 mM KH_2PO_4, 150 mM NaCl, pH 7.4) was delivered into the larval midgut with a 0.25-ml syringe (Yale-BD) fitted with a blunted and polished 30-gauge needle, using a model 1003 Microjector syringe drive and a model 1010 Microdoser (Houston Atlas, Houston, TX). Three sets of 10 larvae were used for each toxin concentration (at least five toxin concentrations were used per toxin), and the dosed larvae were then fed on mulberry leaves. Control insects were dosed with the same volume of phosphate-buffered saline, and the toxicity was assessed after 24 h. Effective dose estimates were obtained by Probit analysis (29).

M. sexta eggs used in this study were supplied by D. L. Dahlman (Dept. of Entomology, University of Kentucky, Lexington). The eggs were hatched and raised on artificial diet (Bio Serve). Toxicity assays were performed with newly hatched larvae as described in Rajamohan *et al.* (23). The mortality rates were recorded after 5 days, and the results were analyzed using probit analysis (29).

The *H. virescens* strain (YDK) used in this study was described in Gould *et al.* (30). Bioassay and data analysis procedures were performed as described previously by Rajamohan *et al.* (23).

Competition Binding Assay—Homologous (competition between labeled and nonlabeled forms of the same ligand) and heterologous (competition between one labeled ligand and another nonlabeled ligand) competition binding assay procedures were as described elsewhere (18). In short, 100 μg/ml BBMV were incubated with 1 nM of labeled toxin and increasing concentrations (0 to 1000 nM) of appropriate nonlabeled toxin in 100 μl of binding buffer at room temperature for 1 h. The pellet was washed three times with binding buffer to remove the unbound toxins, and the radioactivity in the final pellet was measured in a gamma counter (Beckman). Each experiment was repeated at least three times, and the mean values were plotted using the CA-CRICKET Graph III application program. A meticulous kinetic binding study of CryI toxins performed by Liang *et al.* (17) pointed out the inappropriate use of the term K_d (dissociation binding constant), which has been used in previous studies for competition binding of Cry toxins with BBMV (11, 12, 14, 17). In a later study, Wu and Dean (22) used an alternative term, K_{com} for binding constants calculated from competition studies of Cry toxins with BBMV using the LIGAND program (31). Hence, in this study, the term K_{com} will be used in place of K_d. The binding affinity (K_{com}) and binding site concentrations (B_{max}) were calculated using the LIGAND program (31).

Dissociation Binding Assay—Dissociation binding assays were performed essentially as described previously (18). 1.0 nM ^{125}I-labeled toxin was incubated with 200 μg/ml BBMV for 1 h at room temperature (association binding) to achieve saturation binding. Nonlabeled toxin (100 nM, final concentration, in a 20-μl volume) was then added to each sample tube, and the reaction was stopped at different time intervals (5 min to 1 h) by centrifugation. The radioactivity in the pellets was measured in a gamma counter (Beckman).

Voltage Clamp Analysis—The dissection and mounting of *M. sexta* midgut followed the protocol by Harvey *et al.* (32). The amplifier equipment for voltage clamp consisted of a D.C. 1000 voltage/current clamp, an A-310 Accupulser (World Precision Instruments), and a strip chart recorder (Kipp and Zonen). The voltage clamp analysis was performed as described by Rajamohan *et al.* (23). After stabilization of the membrane, trypsin-activated toxin was injected into the lumen side of the gut (final concentration, 50 ng/ml). The I_{sc} (inhibition of short-circuit current) was tracked with a recorder, and data were collected with the MacLab data acquisition system. Each individual experiment was repeated at least three times, and the mean values were plotted using the CA-CRICKET Graph III application program.

RESULTS

Alignment and Construction of Mutants—The alignment of domain II, loop 3, residues of CryIAa toxin (8), with CryIAb toxin are shown in Fig. 1A. Deletion and alanine substitution mutations constructed at the loop 3 region of CryIAa and alanine substitutions of CryIAb loop 3 are shown in Fig. 1B.

Expression and Stability of Mutant Proteins—The δ-endotoxin inclusion bodies purified from wild-type and mutants were solubilized and analyzed on SDS-10% PAGE. All the mutant proteins were expressed in amounts comparable to wild-type (Figs. 2B and 3A). Each also yielded a 60-kDa stable, trypsin-resistant toxin core upon activation with trypsin (Figs. 2A and 3B). To investigate the stability of trypsin-activated toxins with insect gut proteases, the toxins were treated further with gut juice collected from target insects. Western blot analysis showed that all CryIAb (Fig. 2) and CryIAa (Fig. 3) mutant proteins yielded stable 60-kDa toxin, similar to wild-type, upon treatment with *M. sexta* (Figs. 2C and 3D), *H. virescens* (Fig. 2D), and *B. mori* (Fig. 3C), gut juice.

Toxicity and Binding of CryIAb Mutants to M. sexta—The LC$_{50}$, K_{com}, and B_{max} values of CryIAb and mutants S438A, G439A, F440A, S441A, N442A, and S443A toward *M. sexta* were analyzed, and the values are reported in Table I. Mutants G439A and F440A reduced the toxicity (100 and 20 times less, respectively) to *M. sexta*. The LC$_{50}$ values of mutants S438A, S441A, N442A, S443A, and wild-type were 45.5, 10.8, 37.3, and 43.6, and 9.7 ng/cm^2, respectively. These mutants were similar or up to 4 times less potent when compared to the wild-type toxin. The K_{com} of mutants G439A and F440A was 12 and 9 times, respectively, higher than that of CryIAb (Table I). The heterologous binding curves showed that mutant toxins G439A and F440A competed for the binding of labeled wild-type toxin with reduced binding affinity compared to CryIAb, S438A,

S441A, N442A, and S443A toxins (Fig. 4A). Dissociation binding assays with CryIAb, G439A, and F440A labeled toxins showed that about 85–90% of the BBMV-bound toxins were irreversibly associated with the vesicles. However, the total amount of toxin that irreversibly bound to the BBMV was significantly different between the wild-type and the mutants. While 38 ng/mg BBMV of CryIAb toxin was irreversibly associated with the vesicles, only 18 and 15 ng/mg BBMV of F440A and G439A toxins, respectively, were irreversibly bound to *M. sexta* vesicles (Fig. 5).

Response of M. sexta Midgut to CryIAb Mutant Toxins—The voltage clamp experiment measures the active transport of ions across the midgut cells from the hemolymph side to the lumen side. The inhibition of short-circuit current (I_{sc}) illustrates the depolarization of the midgut membrane due to the channel forming activity of Cry toxin. Our experiments showed that the slope of I_{sc} inhibition of CryIAb, S438A, S441A, N442A, and S443A toxins were between −94 to −97 μA/cm^2/min (Table I), whereas the slope for F440A was −60.3 μA/cm^2/min. We were unable to calculate the slope of mutant G439A because of insufficient inhibition of I_{sc} by the mutant toxin at this concentration (Fig. 6).

Binding and Toxicity of CryIAb Mutants to H. virescens—The biological activity of CryIAb and mutant toxins to *H. virescens* were compared and reported in Table II. The LC$_{50}$ of S438A, S441A, N442A, and S443A showed that these mutants were only 2–4 times less toxic (LC$_{50}$ 3.6, 1.6, 1.2, and 2.2 μg/ml diet, respectively) than the wild-type (LC$_{50}$ 0.82 μg/ml diet). In contrast, G439A lost most of its toxicity (insufficient mortality at 15 μg/ml concentration to calculate the exact LC$_{50}$), and F440A reduced the toxicity 15 times compared to wild-type (Table II). The K_{com} estimated by homologous competition assays for wild-type, S438A, S441A, N442A, and S443A toxins were between 3.17 and 5.9 nM (Table II), whereas G439A and F440A were 6–7 times higher (22.33 and 19.97 nM, respectively). In heterologous competition binding studies CryIAb, S438A, S441A, N442A, and S443A toxins competed for binding with higher affinity to *H. virescens* BBMV (Fig. 4B). Mutant toxins G439A and F440A competed with reduced binding affinity (the binding curves were shifted to the right) for the binding sites of labeled wild-type toxin as shown in Fig. 4B. The dissociation binding data with *H. virescens* were similar to that of *M. sexta* reported here, and CryIAb toxin bound 3.7 times more than the mutants G439A and F440A (data not shown).

Insect Bioassay and Binding of CryIAa Mutants—The toxic-

A

```
                β10   Loop 3    β 11
CryIAa  428SHRLSHVTMLS[         ]TLRAPTFSWQHRSAE460
CryIAb  427SHRLSHVSMFRSGFSNSSVSIIRAPMFSWIHRSAE461
```

B

Mutants:

CryIAa

D3a (440-443) 428SHRLSHVTMLSQ----VYTLRAPTFSWQHRSAE460

A3a (437-439) 428SHRLSHVTM**AAA**AAGAVYTLRAPTFSWQHRSAE460

CryIAb

S438A 427SHRLSHVSMFR**A**GFSNSSVSIIRAPMFSWIHRSAE461

G439A 427SHRLSHVSMFRS**A**FSNSSVSIIRAPMFSWIHRSAE461

F440A 427SHRLSHVSMFRSG**A**SNSSVSIIRAPMFSWIHRSAE461

S441A 427SHRLSHVSMFRSGF**A**NSSVSIIRAPMFSWIHRSAE461

N442A 427SHRLSHVSMFRSGFS**A**SSVSIIRAPMFSWIHRSAE461

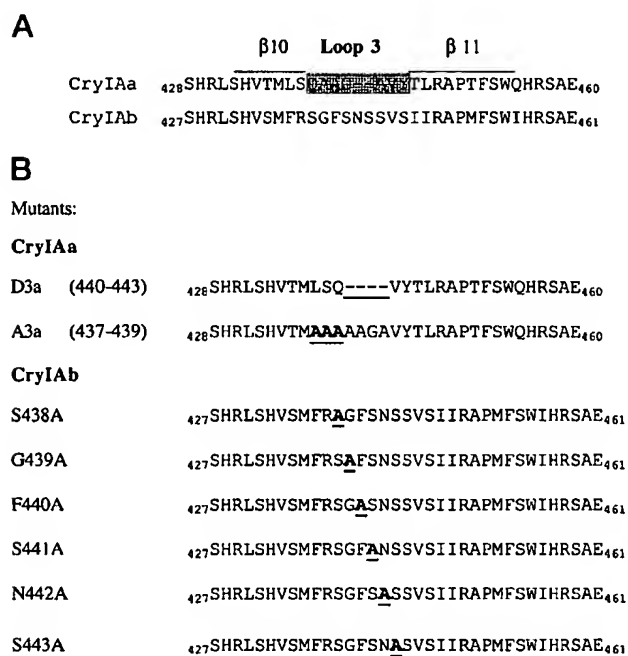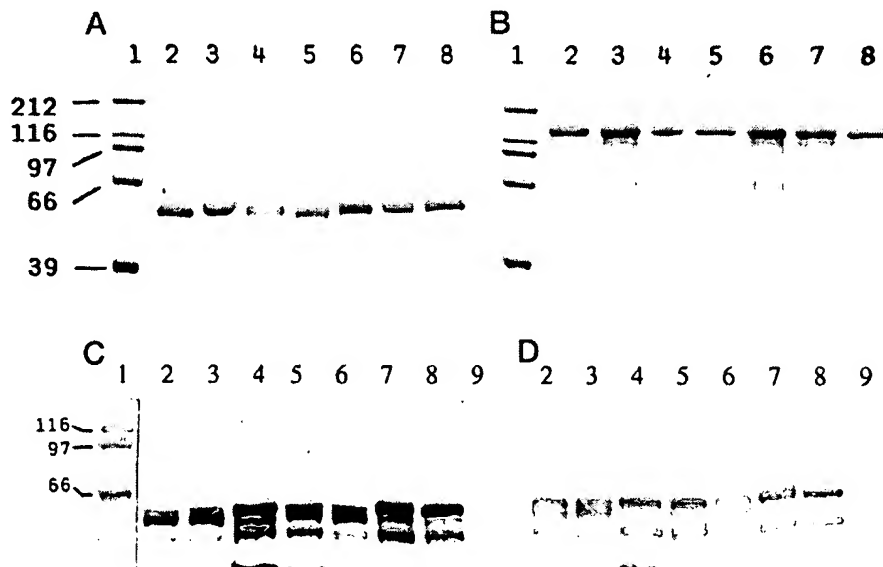S443A 427SHRLSHVSMFRSGFSN**A**SVSIIRAPMFSWIHRSAE461

FIG. 1. *A*, alignment of the toxin protein sequences of CryIAa with CryIAb between residues 427 and 461. The positions of the secondary structural elements of CryIAa are given above its sequence as described by Grochulski *et al.* (8). The loop 3 residues are highlighted. *B*, summary of deletion and alanine substitutions constructed on CryIAa and CryIAb toxins. *A3a*, alanine substitution of CryIAa residues [437]LSQ[439]; *D3a*, deletion of CryIAa residues [440]AAGA[443].

FIG. 2. Coomassie blue-stained SDS-10% PAGE of CryIAb mutants, comparing the yield of trypsin-activated toxins (*A*) protoxins (*B*), Western blot analysis of the stability of wild-type and mutant proteins after digestion with *M. sexta* (*C*) and *H. virescens* (*D*) gut juice. *Lane 1*, molecular mass markers. Masses of the protein markers (in kilodaltons) are shown on the left; *lane 2*, CryIAb; *lane 3*, S438A; *lane 4*, G439A; *lane5*, F440A; *lane 6*, S441A; *lane 7*, N442A; *lane 8*, S443A; and *lane 9*, corresponding insect gut juice.

ity of CryIAa and loop 3 mutant toxins toward *B. mori* and *M. sexta* were analyzed and reported in Table III. The LC$_{50}$ values of A3a to *M. sexta* and *B. mori* (3.1 and 46.3 ng, respectively) were similar to the wild-type toxin (2.5 and 40.5 ng, respectively). Whereas the mutant D3a is about 28 times less toxic to *M. sexta* and >62 times less toxic to *B. mori* when compared to the wild-type toxin (Table III).

The binding affinity (K_{com}) and binding site concentrations (B_{max}) of CryIAa and mutant toxins to midgut vesicles prepared from *B. mori* and *M. sexta* were calculated by homologous competition binding assays, and the results were shown in Table III. The K_{com} and B_{max} value of the mutant A3a was comparable with CryIAa for both the insects, whereas the K_{com} value of D3a was about 15 and 9 times higher than CryIAa, for *M. sexta* and *B. mori*, respectively, representing reduced binding affinity (Table III). When the wild-type toxin was labeled with ^{125}I and put into competition with nonlabeled wild-type or mutant toxins, CryIAa and A3a displayed higher affinity binding to *B. mori* and *M. sexta* (Fig. 7, *A* and *B*), whereas the D3a curve was shifted to the right compared with that of CryIAa or A3a to both insect BBMV (Fig. 7, *A* and *B*).

DISCUSSION

Elucidation of the mechanism of interaction between the δ-endotoxin and insect midgut receptor(s) is critical to the rational design of improved insecticidal toxins with broader insect specificity and higher larvicidal potency. The insect specificity determining region of CryI type toxins has been located primarily in domain II for several lepidopterans (26, 33, 34). The three-dimensional structure of CryIAa suggests that the apex of domain II is composed of three solvent-exposed loops comprising residues 310–313 (loop 1), 367–379 (loop 2), and 438–446 (loop 3). The striking dissimilarity between CryIAa and CryIAb toxins in amino acid sequences in loops 2 and 3 inspired us to investigate the role of these residues in insect specificity, toxicity, and receptor binding.
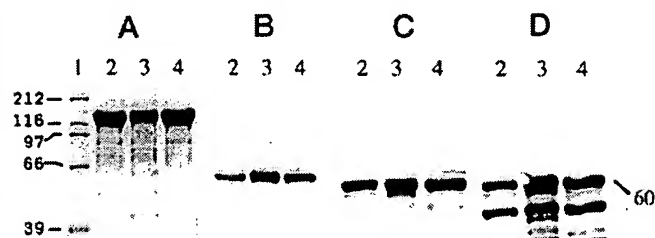
Although CryIAa and CryIAb share 89% overall amino acid sequence identity and bind to the same receptor (210 kDa) in the gypsy moth, loop 3 residues of domain II are significantly different (Fig. 1). In this study, loop 3 residues, [438]SGFSNS[443], of CryIAb toxin were individually replaced with alanine and tested for toxicity to *M. sexta* and *H. virescens*. Our bioassay

FIG. 3. **Coomassie blue-stained SDS-10% PAGE of CryIAa mutants, comparing the yield of protoxins** (*A*) **trypsin-activated toxins** (*B*), **Western blot analysis of the stability of wild-type and mutant proteins after digestion with *B. mori*** (*C*) **and *M. sexta*** (*D*) **gut juice.** *Lane 1*, molecular mass markers. Masses of the protein markers (in kilodaltons) are shown on the left; *lane 2*, CryIAa; *lane 3*, A3a; and *lane 4*, D3a.
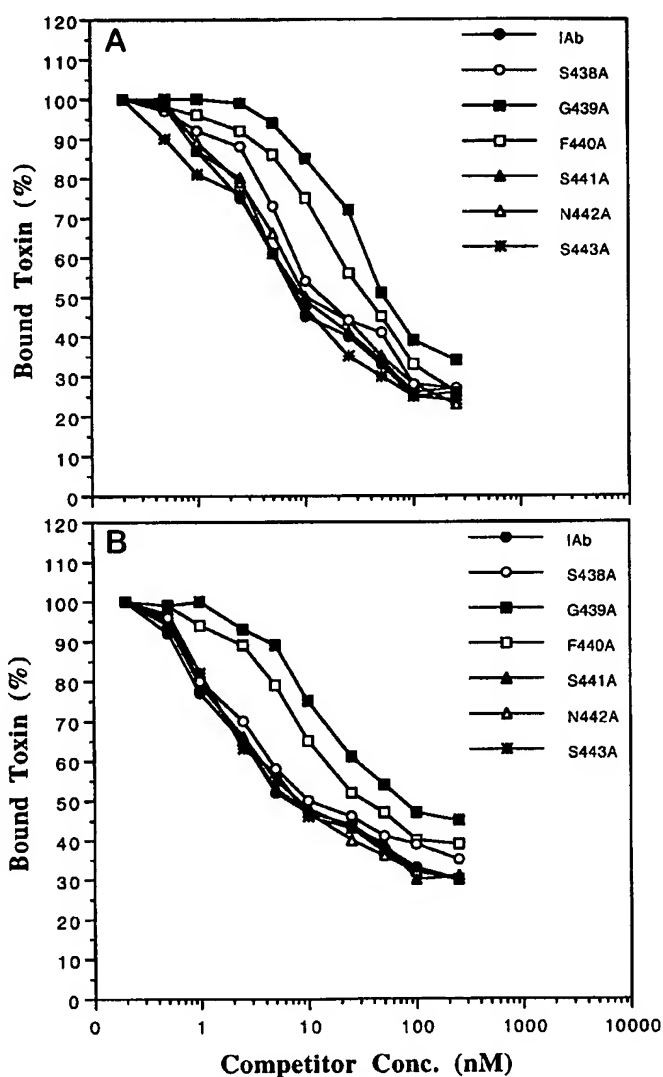
FIG. 4. **Binding of ^{125}I-labeled (1 nM) CryIAb toxin in the presence of increasing concentrations of nonlabeled CryIAb, S438A, G439A, F440A, S441A, N442A, and S443A toxins to *M. sexta*** (*A*) **and *H. virescens* BBMV** (*B*). Binding is expressed as a percentage of the total amount bound upon incubation with labeled toxin alone. On *M. sexta* and *H. virescens* vesicles, the amount is 2400 ± 80 cpm and 2250 ± 35 cpm, respectively for CryIAb.

TABLE I

Insecticidal activity, binding affinity, and I_{SC} inhibition of CryIAb mutant proteins to M. sexta

Toxins	LC$_{50}$[a]	K_{com}[b]	B_{max}[c]	I_{SC} inhibition rate[d]
	ng/cm²	*nM*	*pmol/mg*	*μA/cm²/min*
CryIAb	9.7 (6.2–14)	1.8 ± 0.55	4.05 ± 0.4	−97.4 ± 5.6
S438A	45.5 (37–61)	2.77 ± 0.71	5.25 ± 0.2	−93.1 ± 4.9
G439A	1000 (920–1300)	21.0 ± 2.70	9.05 ± 1.1	UD[e]
F440A	190 (155–222)	16.1 ± 3.11	8.11 ± 1.7	−60.3 ± 4.1
S441A	10.8 (6.5–16)	1.9 ± 0.31	4.91 ± 0.7	−94.1 ± 5.2
N442A	37.3 (26–51)	3.0 ± 0.71	4.99 ± 0.8	−93.9 ± 8.9
S443A	43.6 (36–53)	2.69 ± 0.84	5.79 ± 0.7	−94.3 ± 3.1

[a] LC$_{50}$, 50% lethal concentration, 95% confidence intervals are given in parentheses.
[b] K_{com}, dissociation constant (determined from homologous competition binding). Each value is the mean of three individual experiments.
[c] B_{max}, binding site concentration (determined from homologous competition binding). Each value is the mean of three experiments.
[d] Each value if the mean of three experiments.
[e] Undetectable.

data show that the mutants G439A (alanine replacement of Gly[439]) and F440A have substantially reduced toxicity to *M. sexta* (100 and 20 times, respectively) and *H. virescens* (>15 times). The other mutants (S438A, S441A, N442A, and S443A) only marginally affected toxicity. Evidence such as 1) expression of mutant toxins at levels comparable to wild-type (Fig. 2*B*), 2) stability of the mutant toxins (60 kDa) upon digestion with trypsin (Fig. 2*A*), and 3) processing wild-type and mutant toxins alike into 60-kDa toxin by insect gut enzyme digestion (Fig. 2, *C* and *D*) suggest that the loss of toxicity was not caused by instability of mutant toxins in the insect midgut. It was noticed that the digestion of mutant toxins, especially G439A, with *M. sexta* and *H. virescens* gut juice generated a few minor peptides in addition to the stable 60-kDa toxin, suggesting that G439A might be slightly more susceptible to insect gut pro-

teases than the wild-type. However, we do not expect this to account for the substantial loss of toxicity of G439A (100 and >12 times for *M. sexta* and *H. virescens*, respectively) to the test insects, since these minor peptides were also observed in the mutants (S441A, N442A, and S443A) which are relatively as toxic as the wild-type. Competition binding assays revealed that the K_{com} of wild-type and toxic mutants (S438A, S441A, N442A, and S443A) did not differ for either of the insect (Tables I and II). In contrast, the K_{com} of G439A and F440A were considerably higher than wild-type with *M. sexta* (12 and 9 times, respectively) and *H. virescens* (7 and 6 times, respectively), suggesting lower binding affinity of these mutants to midgut membrane vesicles (Fig. 4, *A* and *B*). These results correlate with our bioassay data that toxins with higher potency (CryIAb, S438A, S441A, N442A, and S443A) exhibit higher affinity binding, whereas toxins with marginal potency (G439A and F440A) show weaker binding. Our dissociation binding assays showed that alanine substitution of Gly[439] and Phe[440] did not affect the off-rate of the BBMV-bound toxin since 85–90% of bound wild-type and mutants (G439A and F440A) were irreversibly associated to the midgut vesicles prepared from both target insects. By comparison to wild-type toxin in both target insects, mutants G439A and F440A showed 3.5-fold reduction in the amount bound (Fig. 5). The marginal potency in bioassay exhibited by mutants G439A and F440A is consistent with the initial binding analyses showing that midgut vesicles from both target insects show reduced numbers of mutant toxins bound as well as lowered binding affinity. We also examined the inhibition of I_{sc} across the isolated midgut in response to the addition of wild-type and mutant toxins. The toxins that have higher binding affinity to the receptor inhibit the I_{sc} more efficiently than the toxins with reduced binding affinity (Fig. 6).
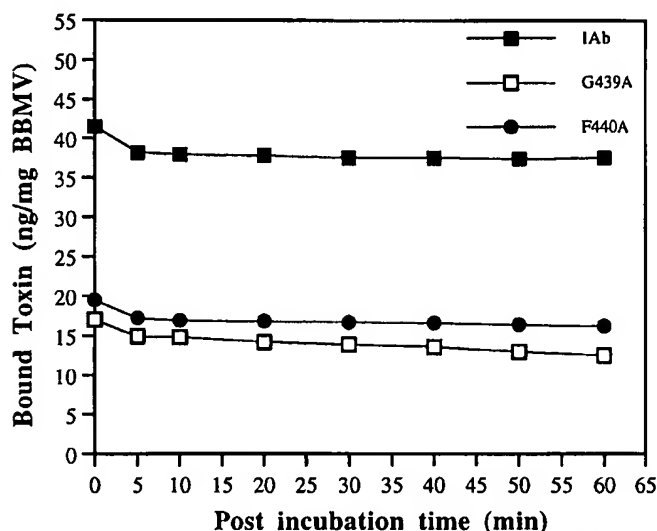
The involvement of CryIAb, loop 3 Gly residue (Gly[439]) in initial receptor binding toward *H. virescens* is in agreement with our previous observation that when loop 2, Gly[374], was mutated to Ala, it reduced the initial binding to *H. virescens* BBMV (23). The loss of toxicity of G439A could be argued as a result of minor changes in the flexibility of the loop, since Gly promotes turns and mobility of loops (35). Therefore, it may

FIG. 5. **Dissociation of bound ¹²⁵I-labeled toxins from *M. sexta* BBMV.** *M. sexta* BBMVs (200 μg/ml) were incubated with 1 nM ¹²⁵I-labeled CryIAb, G439A, and F440A toxins for 1 h (association reaction). After the association reaction, 100 nM corresponding nonlabeled toxins were added to the test samples, and incubation was continued (post-binding incubation). Binding is expressed as nanograms of toxin bound/mg of BBMV.

FIG. 6. **Inhibition of I_{sc} across *M. sexta* midgut.** A total of 50 ng/ml CryIAb, S438A, G439A, F440A, S441A, N442A, and S443A toxin were injected in separate experiments into the lumen side of the chamber, and the drop in I_{sc} was measured. The I_{sc} measured before the addition of the toxin is considered as 100%.
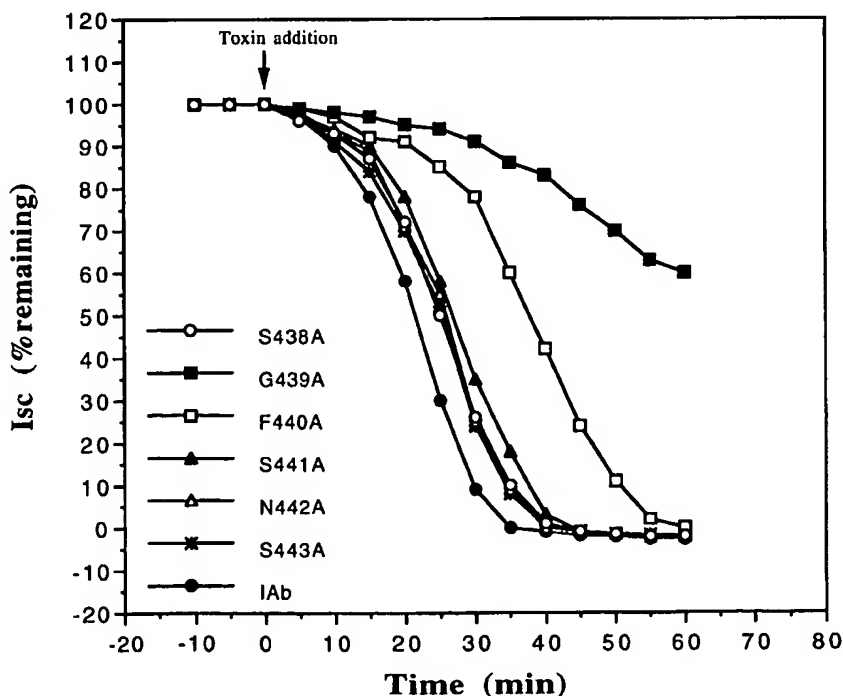
TABLE II

Biological activity and binding affinity of CryIAb mutant proteins toward H. virescens

Toxin	LC_{50}^a	K_{com}^b	B_{max}^c
	μg/ml	nM	pmol/mg
CryIAb	0.82 (0.4–1.5)	3.17 ± 0.21	30.51 ± 3.5
S438A	3.61 (2.2–6.2)	4.21 ± 0.80	34.25 ± 3.1
G439A	>15	22.33 ± 2.31	42.01 ± 2.7
F440A	12.44 (6.4–26)	19.97 ± 3.11	44.91 ± 3.3
S441A	1.6 (0.9–2.9)	5.91 ± 0.27	29.39 ± 2.8
N442A	1.2 (0.5–5.3)	3.01 ± 0.99	31.66 ± 1.9
S443A	2.2 (1.3–3.6)	4.99 ± 1.11	28.98 ± 2.6

[a] LC_{50}, 50% lethal concentration, 95% confidence intervals are given in parentheses.

[b] K_{com}, dissociation constant (determined from homologous competition binding). Each value is the mean of three individual experiments.

[c] B_{max}, binding site concentration (determined from homologous competition binding). Each value is the mean of three experiments.

TABLE III

Insecticidal activity and binding constants of CryIAB mutant proteins to M. sexta and B. mori

Toxin	LC_{50}^a	K_{com}^b	B_{max}^c
	ng/cm²	nM	pmol/mg
M. sexta			
CryIAb	2.5 (1.1–4.5)	1.17 ± 0.5	20.51 ± 3.5
A3a	3.1 (1.5–5.1)	3.21 ± 0.8	24.25 ± 3.9
D3a	70.5 (61–89)	10.30 ± 1.3	110.0 ± 7.7
B. mori	LD_{50}^d		
	(ng/larvae)		
CryIAa	40.5 (32.1–51.8)	0.8 ± 0.05	15.25 ± 3.4
A3a	46.3 (39.1–55.7)	1.77 ± 0.2	21.25 ± 4.1
D3a	>2,500	12.0 ± 1.7	95.05 ± 6.8

[a] LC_{50}, 50% lethal concentration, 95% confidence intervals are given in parentheses.

[b] K_{com}, dissociation constant (determined from homologous competition binding). Each value is the mean of three individual experiments.

[c] B_{max}, binding site concentration (determined from homologous competition binding).

[d] LD_{50}, 50% lethal dose, 95% confidence intervals are given in parentheses. Each value is the mean of three experiments.

FIG. 7. **Binding of** ^{125}I-labeled (1 nM) CryIAa toxin in the presence of increasing concentrations of nonlabeled CryIAa, A3a, and D3a toxins to *B. mori* BBMV (*A*) and *M. sexta* BBMV (*B*). Binding is expressed as a percentage of the total amount bound upon incubation with labeled toxin alone. The amount for CryIAa is 1380 ± 50 cpm and 2100 ± 45 cpm on *B. mori* and *M. sexta* vesicles, respectively.

indirectly affect binding affinity. Phe at loop 3 plays a critical role in toxicity and receptor binding, similar to the role in loop 2 (18), but its effect on binding is significantly different in the two loops. Alanine substitution of Phe[371] at CryIAb loop 2 did not have any effect on initial receptor binding, but extensively affected the irreversible association of the toxin to the BBMV and dramatically reduced (400 times less) the toxicity to *M. sexta* (18). In contrast, alanine substitution of Phe[440] (a stronger hydrophobic residue than alanine) in the loop 3 affected the initial binding of the toxin to the same insect. This may suggest that Phe plays functionally distinct roles (initial binding and irreversible binding to *M. sexta*) when located at different loops of CryIAb toxin. Furthermore, alanine substitution of two positively charged residues at loop 2 ([368]RR[369]) eliminates the initial binding of the toxin almost completely with *M. sexta* BBMV (23). Considering these results, we propose that the initial receptor recognition process of the toxin is a combination of charge (loop 2) and hydrophobic (loop 3) interactions.

To further examine the functional role of hydrophobic residues, we mutated the loop 3 residues of CryIAa. We have constructed two mutants, A3a (alanine substitution of residues [437]LSQ[439]) and D3a (deletion of [440]AAGA[443]). Digestions with trypsin and insect (*B. mori* and *M. sexta*) gut juice enzyme (the ultimate environment that determines the stability of the toxin) showed that the mutant proteins were as stable as the wild-type toxin (Fig. 3, *B–D*). Further studies with A3a on insect toxicity and binding revealed that this mutant affected neither toxicity nor binding for *B. mori* and *M. sexta*, which are highly susceptible to CryIAa toxin (Table III, Fig. 7, *A* and *B*).
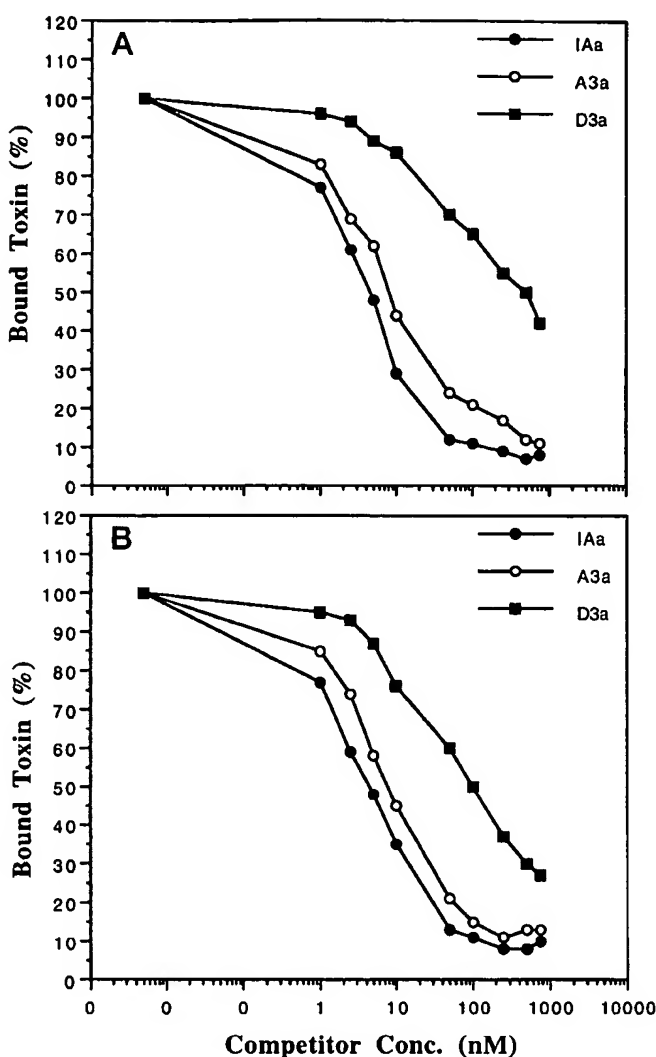
Since the residues [437]LSQ[439] are located between β10 and loop 3, they might not be completely exposed for the interaction with the receptor. On the contrary, D3a reduced the toxicity >68 times to *B. mori* and 28 times to *M. sexta* (Table III). Binding experiments with insect midgut vesicles showed that the deletion of relatively hydrophobic loop residues [440]AAGA[443] (D3a) disrupted binding affinity (K_{com}) by 15 times to *B. mori* and 9 times to *M. sexta* (Table III). Hence, it is reasonable to speculate that the reduced potency of D3a to both insects is attributable to the reduced initial binding affinity. These experiments suggest that the loop 3 residues (440–443) of CryIAa contain important binding determinants to *B. mori* and *M. sexta* receptor(s). Considering the lack of any active side chain among the loop 3 residues, [440]AAGA[443], the stretch of alanines might provide hydrophobicity, and their deletion could remove a hydrophobic interaction. Consequently, the studies with CryIAa also support our earlier proposal that the hydrophobic residues of loop 3 are important for initial receptor binding. We have previously reported that a deletion of charged and hydrophobic loop 2 residues ([365]LYRRIIL[371]) of CryIAa resulted in substantial loss of initial binding and toxicity to *B. mori* (24). It is obvious from these studies that in both CryIAa and CryIAb

toxins charge (loop 2) and hydrophobicity (loops 2 and 3) play a key role in initial receptor binding.

Our experiments do not exclude the possibility that the toxins (CryIAa and CryIAb) bind to two different binding sites on the same receptor, one with higher binding affinity and the other with lower affinity. In that case, the loop 3 mutations selectively affected a higher affinity site that is important for toxicity. These results provide evidence that the receptor binding residues of these toxins are physically scattered, rather than clustered in a confined region of the toxin. Recent studies with domain swapping experiments suggest that domain III, in addition to domain II, is involved in insect specificity and receptor recognition (13, 36). As a result, these loops are excellent targets for genetic redesigning of novel toxins with diverse specificity by exchanging the residues or chain lengths of the active site without affecting the structural frame work of the toxin.

REFERENCES

1. Feitelson, J. S., Payne, J., and Kim, L. (1992) *Bio/Technology* 10, 271–275
2. Yamamoto, T., and Powell, G. K. (1993) in *Advanced Engineered Pesticides* (Kim, L., ed) pp. 3–42, Marcel Dekker, New York
3. Hofmann. C., Lüthy, P., Hutter, R., and Pliska, V. (1988) *Eur. J. Biochem.* 173, 85–91
4. Lee, M. K., Milne, R. E., Ge, A. Z., and Dean, D. H. (1994) *J. Biol. Chem.* 267, 3115–3121
5. Knowles, B. H., and Ellar, D. J. (1987) *Biochim. Biophys. Acta* 924, 509–518
6. Wolfersberger, M. G. (1989) *Arch. Insect Biochem. Physiol.* 12, 267–277
7. Schwartz, J.-L., Garneau, L., Masson, L. and Brousseau, R. (1991) *Biochim. Biophys. Acta* 1065, 250–260
8. Grochulski, P., Masson, L., Borisova, S., Pusztai-Carey, M., Schwartz, J. L., Broysseau, R., and Cygler, M. (1995) *J. Mol. Biol.* 254, 447–464
9. Li, J., Carroll, J., and Ellar, D. J. (1991) *Nature* 353, 815–821
10. Wu, D., and Aronson, A. I. (1992) *J. Biol. Chem.* 267, 2311–2317
11. Chen, X. J., Curtiss, A., Alcantara, E., and Dean, D. H. (1995) *J. Biol. Chem.* 270, 6412–6419
12. Chen, X. J., Lee, M. K., and Dean, D. H. (1993) *Proc. Natl. Acad. Sci. U. S. A.* 90, 9041–9045
13. Lee, M. K., Young, B. A., and Dean, D. H. (1995) *Biochem. Biophys. Res. Comun.* 216, 306–312
14. Nishmoto, T., Yoshisue, H., Ihara, K., Sakai, H., and Komano, T. (1994) *FEBS Lett.* 348, 249–254
15. Van Rie, J., McGaughey, W. H., Johnson, D. E., Barnett, B. D., and Van mellaert, H. (1990) *Science* 247, 72–74
16. Ferré, J., Real, M. D., Van Rie, J., Jansens, S., and Peferoen, M. (1991) *Proc. Natl Acad. Sci. U. S. A.* 88, 5119–5123
17. Liang, Y., Patel, S. S., and Dean, D. H. (1995) *J. Biol. Chem.* 270, 24719–24724
18. Rajamohan, F., Alcantara, E., Lee, M. K., Chen, X. J., and Dean, D. H. (1995) *J. Bacteriol.* 177, 2276–2282
19. Sangadala, S., Walters, F. S., English, L. H., and Adang, M. J. (1994) *J. Biol. Chem.* 269, 10088–10092
20. Vadlamudi, R. K., Ji, T. H., and Bulla, L. A., Jr. (1991) *J. Biol. Chem.* 268, 12334–12340
21. Lee, M. K., and Dean, D. H. (1996) *Biochem. Biophys. Res. Commun.*, 220, 575–580
22. Wu, S. J., and Dean, D. H. (1996) *J. Mol. Biol.* 255, 628–640
23. Rajamohan, F., Cotrill, J. A., Gould, F., and Dean, D. H. (1996) *J. Biol. Chem.* 271, 2390–2396
24. Lu, H., Rajamohan, F., and Dean, D. H. (1994) *J. Bacteriol.* 176, 5554–5559
25. Kwak I. S., Lu, H., and Dean, D. H. (1995) *Mem. Inst. Oswaldo Cruz Rio J.* 90, 75–79
26. Ge, A. Z., Shivarova, N. I., and Dean, D. H. (1989) *Proc. Natl. Acad. Sci. U. S. A.* 86, 17954–17958
27. Sanger, F. A., Nicklen, A., and Coulson, A. R. (1977) *Proc. Natl. Acad. Sci. U. S. A.* 74, 5463–5467
28. Wolfersberger, M. G., Lüthy, P., Maure, A., Parenti, P., Sacchi, V. F., Giordana, B., and Hanozet, G. M. (1987) *Comp. Biochem. Biophysiol.* 86A, 301–308
29. Raymond, M. (1985) *Entomol. Mer. Parasitol.* 22, 117–121
30. Gould, F., Anderson, A., Reynolds, A., Bumgarner, L., and More, W. (1995) *J. Econ. Entomol.* 88, 1545–1559
31. Munson, P. J., and Rodbard, D. (1980) *Anal. Biochem.* 107, 220–239
32. Harvey, W. R., Crawford, D. N., and Spaeth, D. D. (1990) *Methods Enzymol.* 192, 599–608
33. Masson, L., Mazza, A., Gringorten, J. L., Baines, D., Anelunias, V., and Brousseau, R. (1994) *Mol. Microbiol.* 14, 851–860
34. Schnepf, H. E., Tomczak, K., Ortega, J. P. and Whiteley, H. R. (1990) *J. Biol. Chem.* 265, 20923–20930
35. Ramachandra, G. N., and Sassiekharan, V. (1968) *Adv. Prot. Chem.* 28, 283–437
36. Bosch, D., Schipper, B., van der Kleij, H., de Maagd, R. A., and Stekema, W. J. (1994) *Bio/Technology* 12, 915–919